Original Article Clinics in Orthopedic Surgery 2025;17:204-215 • https://doi.org/10.4055/cios24194

Additional Screw Added to the Femoral Neck System Could Enhance the Stability of Pauwel Type III Femoral Neck Fractures: a Finite Element Analysis

Yonghan Cha, MD, Sunghoon Park, MD*, Chang-Ho Jung, PhD†, Jin-Woo Kim, MD‡, Jun-Il Yoo, MD§, Jung-Taek Kim, MD‖, Yongho Jeon, PhD†, Kyeong Jin Han, MD‖

Department of Orthopedic Surgery, Daejeon Eulji Medical Center, Eulji University School of Medicine, Daejeon,
**Department of Radiology, Ajou University Medical Center, Ajou University School of Medicine, Suwon,*
†Department of Mechanical Engineering, Ajou University, Suwon,
‡Department of Orthopedic Surgery, Nowon Eulji Medical Center, Eulji University School of Medicine, Seoul,
§Department of Orthopedic Surgery, Inha University Hospital, Inha University School of Medicine, Incheon
‖Department of Orthopedic Surgery, Ajou University Medical Center, Ajou University School of Medicine, Suwon, Korea

Background: This study explores effective fixation methods for Pauwel type III femoral neck fractures by evaluating the biomechanical benefits of adding a screw to the Femoral Neck System (FNS).

Methods: Computed tomography (CT) scans of an 82-year-old female patient with an intertrochanteric fracture were used to establish a finite element femur model with heterogeneous material properties. Finite element models of Pauwel type III fractures were created with and without an additional screw. The central and inferior trajectories of the FNS bolt were examined separately and combined with an additional screw for virtual fixation. Walking and stair-climbing loads were applied.

Results: With the addition of a screw, both peak maximum and minimum principal strains consistently stayed comparable or decreased in models with both central and inferior bolt trajectories, while the volume of elements with principal strain exceeding 1% decreased by more than half. The peak von Mises stress observed in the implants ranged from 215.7 to 359.3 MPa, remaining below the titanium alloy's yield strength of 800 MPa. For normal walking, the addition of a screw to the central bolt trajectory model decreased the fracture gap by 50.6% and reduced sliding distance by 8.6%. For the inferior bolt trajectory, the gap was reduced by 57.9% and sliding distance by 25.0%. Under stair-climbing conditions, these improvements were also evident; the central trajectory model saw a halved fracture gap and a 7.9% decrease in sliding distance, while the inferior trajectory model experienced a 55.7% gap reduction and a 27.2% decrease in sliding distance. The additional screw increased the area ratio of the fracture site experiencing interfragmentary compression 34%–39%, while the additional screw alleviated peak interfragmentary compression by 12%–18% under both normal walking and stair-climbing conditions.

Conclusions: The addition of a screw reduced the fracture gap, sliding distance, and peak interfragmentary compression, while increasing the area ratio of interfragmentary compression under both walking and stair-climbing loads, regardless of the FNS bolt trajectory, suggesting a better mechanical environment for fracture healing.

Keywords: *Femoral neck fractures, Finite element analysis, Biomechanical phenomena, Orthopedic fixation devices, Fracture fixation*

Received May 9, 2024; Revised August 2, 2024; Accepted August 2, 2024

Correspondence to: Jung-Taek Kim, MD
Department of Orthopedic Surgery, Ajou University Medical Center, Ajou University School of Medicine, 164 World cup-ro, Yeongtong-gu, Suwon 16499, Korea
Tel: +82-31-219-5220, Fax: +82-31-219-5229, E-mail: orthopedist7@ajou.ac.kr
Yonghan Cha and Sunghoon Park contributed equally to this work as co-first authors.

Due to potential complications such as nonunion and femoral head osteonecrosis, the treatment of femoral neck fractures poses a significant challenge.[1] Currently, 3 methods of fixation are commonly utilized for femoral neck fractures.[2] The first method is multiple cannulated screws fixation, which is commonly employed for fragility fractures.[3] The second method involves the use of a dynamic hip screw (DHS) for femoral neck fractures in the younger population with high-energy injuries.[4] The third method involves the Femoral Neck System (FNS; DePuy Synthes), which is a relatively recent and promising fixation method.[2,5,6] The first 2 devices have been traditionally utilized; extensive experience with these techniques has been acquired, resulting in various techniques and reported outcomes. For example, in multiple cannulated screws fixation, it is recommended to maximize the distance between the screws and position them to support the endocortex of the femoral neck.[3] In the case of DHS, additional antirotation screws are suggested to enhance the rotational stability of the head.[7] Conversely, the experience acquired with FNS is comparatively limited. Although the manufacturer provides standardized surgical techniques, researchers continue to explore various approaches to achieve more robust fixation under specific conditions, contributing to the evolution of standard methods.[8-10]

To investigate a potentially more stable fixation method using the FNS, it would be efficient to assess the effects by applying techniques that have been previously recommended for traditional devices. Given the structural similarity between the DHS and FNS, the use of an additional screw could also be applied to the FNS.[7] Similarly, the practice of widening the distance between screws could be applied to the FNS by widening the distance between the FNS and the additional screw.[3]

In this study, we hypothesized that the addition of a screw to the FNS could enhance stability at the fracture site and that increasing the distance between the FNS and the screw could result in improved fixation stability. Therefore, this study aimed to analyze the stability of FNS fixation with and without an additional screw and to compare the mechanical properties at the fracture site based on the presence of an additional screw using the finite element models of Pauwel type III femoral neck fractures.

METHODS

The requirement for informed consent was waived, and the study protocol was approved by the Institutional Review Board of Ajou University Hospital (IRB No. AJOUIRB-DB-2023-074). All methods in the study were carried out in accordance with the Helsinki Guidelines and Declaration.

Implant Model

To create the implant model, FNS was scanned using the micro-computed tomography (CT; SkyScan1173; Bruker-CT) and images were processed into tomographic images using NRecon (Bruker-CT). These inputs were then employed to design the model using Solidworks 2019 (Dassault System). Through an iterative process of comparing and modifying the engineered model with the STL model, a close approximation of the engineered model to the STL model was established. A 3-dimensional computer-aided design format file of a cannulated screw with a 6.5-mm thread diameter (TDM) was provided by the manufacturer.

Three-dimensional Modeling of the Femur

The coordinate system established by Bergmann et al. and centered around the femur was employed in this study.[11] This osteoporotic femur model was created using CT scans of the femur, specifically that of the left pertrochanteric fracture of an 82-year-old female patient. The patient had a height of 160 cm and a weight of 54 kg. To generate 3-dimensional (3D) models of the intact right femur from the CT images, the Materialise Interactive Medical Image Control System Research 22.0 (MIMICS; Materialise) was utilized.

Fracture Models

Using 3-Matic 14 software (Materialise), a virtual osteotomy was performed to create a model of a Pauwels type III femoral neck fracture.[12] The fracture plane was set at a 60° angle to the horizontal plane, assuming a complete anatomical reduction without any fracture gap.[12]

Meshing

The finite element models were meshed using 10-node tetrahedral elements, ensuring that all elements were smaller than 1 mm. On average, each model consisted of 6,652,731 nodes and 4,824,461 elements.

Implant Positioning

The 3D-fractured femur model was virtually fixed with the 3D implant model using 3-Matic software. For models with central and inferior bolt trajectory, a virtual assembly was created, consisting of a 90-mm long bolt, a 90-mm long anti-rotation screw, a 2-hole plate, and 2 locking screws. The length of the bolt was determined to ensure that the bolt tip would be positioned within a range of 5–10 mm from the subchondral bone.[13] In the models with an inferior trajectory, the inferior surface of the bolt made contact with the endocortical bone, defined as voxels with

over 400 Hounsfield units (HU).[14] Voxels with HU below 400 were considered to be the trabecular bone.

To establish screw-added models with central and inferior trajectories, a partially threaded cannulated screw with a 6.5-mm thread diameter was added to the models with central and inferior bolt trajectories, respectively. The path of the cannulated screw touched the anterosuperior endocortex of the femoral neck (Fig. 1). For clarity and brevity in descriptions, each fixation method was assigned a concise symbol. The bolt trajectories were differentiated into central and inferior, and the models were marked with "+screw" for those including an additional screw and "-screw" for those without it. Thus, the "central FNS + screw" model refers to the finite element model of a femoral neck fracture fixed with an FNS in the central bolt trajectory including an additional screw, and the "inferior FNS + screw" model refers to the model with an FNS in the inferior bolt trajectory including an additional screw. The bone loss resulting from the drilling, reaming, and tapping processes during the insertion of the FNS and the cannulated screw was replicated using Boolean subtraction to mimic the post-fixation construct (Fig. 1).[10]

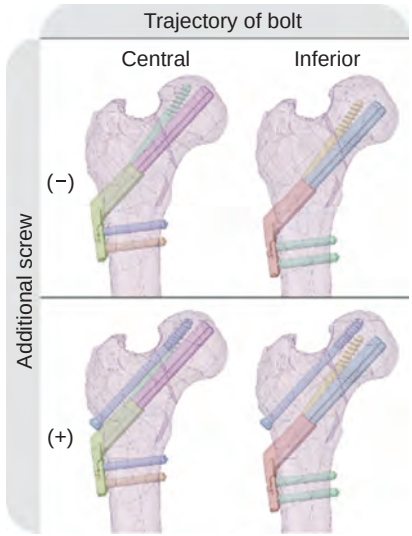

Fig. 1. Pauwels type III femoral neck fracture finite element models were virtually fixed with the Femoral Neck System (FNS) in the central and inferior trajectories of a bolt with and without an additional screw. In total, 4 different combinations of surgical variations of the FNS were established. The models in the upper row were fixed with FNS alone and indicated as "–screw." Those in the lower row had an additional screw and were indicated as "+screw." The models in the left column had the central trajectory of a bolt and were indicated as "central FNS." Those in the right column had the inferior trajectory and were indicated as "inferior FNS."

Boundary Conditions

The contact between the simplified models of the locking screws in the femoral diaphysis was considered to have an infinite friction coefficient. The interfaces between (1) the bolt and anti-rotation screw and (2) the plate and the locking screws were assumed to be bonded. Frictional contact was assumed for all other interfaces between the implant and the 2 fracture fragments. The friction coefficients assigned were 0.46, 0.42, and 0.20 for bone-bone, bone-implant, and implant-implant interfaces, respectively.[15] The distal articular surface of the femur was fixed within the world coordinate system.

Properties of the Materials

The material properties of the bone elements were determined using the mapping approach based on the research

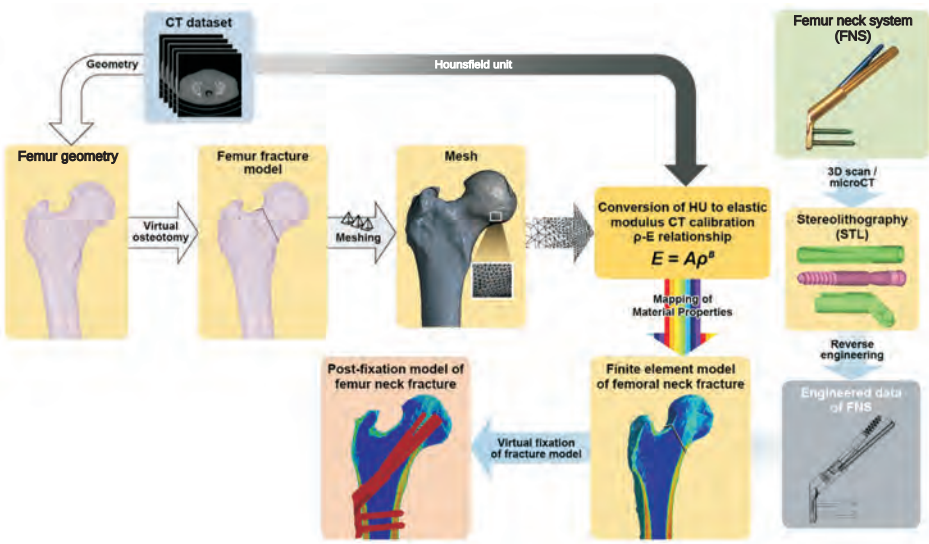

Fig. 2. Each femur element was given the material property of the matched voxels of the computed tomography (CT) scan by calculating Hounsfield units (HU).

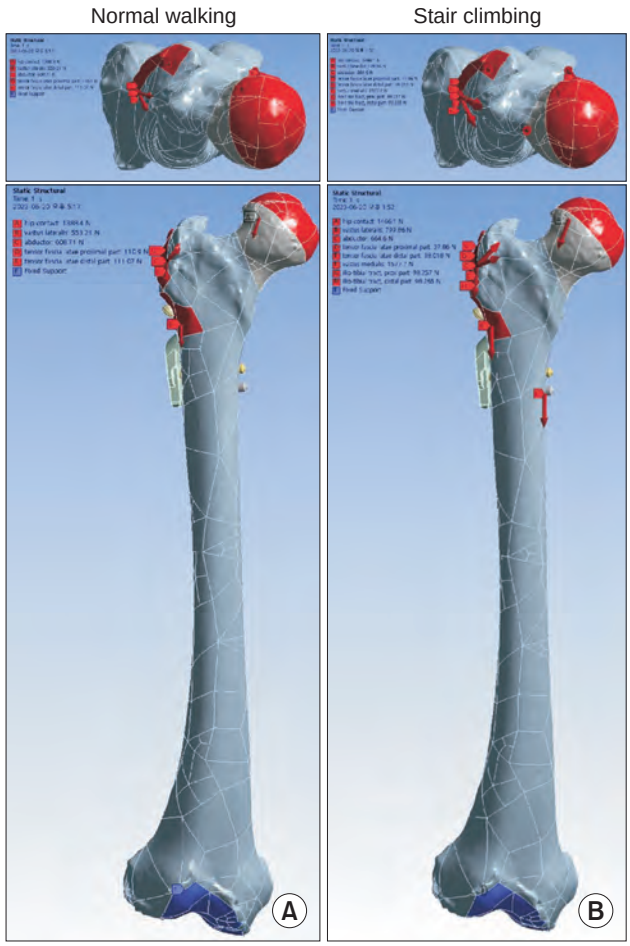

Fig. 3. Fracture models were virtually loaded in the normal walking (A) and stair-climbing (B) conditions. Weight load was transferred to the hemispheric surface of the femoral head at an inclination of 45° and retroversion of 25° in consideration of the abduction of the acetabulum and the combined anteversion of the acetabulum and femoral neck. The distal articular face of the femur was set to be fixed in the world coordinate system.

conducted by Morgan et al.[16,17] This approach involved a series of steps, including matching the CT HU to ash density, then to apparent density, and finally to Young's modulus. A total of 1,800 groups were created to assign the material properties of the bones, as shown in Fig. 2. The assumed Poisson's ratio for the bone elements was 0.3.[17] The metal implants were assigned the material properties of the titanium alloy (Ti-6Al-7Nb), which included an elastic modulus of 105 GPa, Poisson's ratio of 0.34, and a yield strength of 800 MPa.[18] All materials were assumed to have isotropic and linear elastic properties.

Loading Condition

In accordance with Bergmann et al.'s approach, all the models were subjected to loads corresponding to normal walking and stair-climbing conditions.[11] Among the daily activities considered for the load on the hip joint, excluding static activities such as sitting, standing, or lying down, these activities account for the highest proportion.[19] These forces were applied at the insertion or origin site of the hip abductor, tensor fascia latae, iliotibial band, vastus medialis, and vastus lateralis (Fig. 3).[20,21]

Comparative Parameters

The maximum and minimum principal strains were calculated for the femoral elements to assess the potential risk of mechanical failure of the bone.[22] The cut-off for principal strain was set at 1.0% for maximum principal strain and –1.0% for minimum principal strain.[23-25] The total volume of elements with principal strain exceeding a cutoff level was provided.[24,26] The von Mises stress (VMS) was evaluated for the metal implants to assess the risk of mechanical failure of implant. The interfragmentary gap and sliding

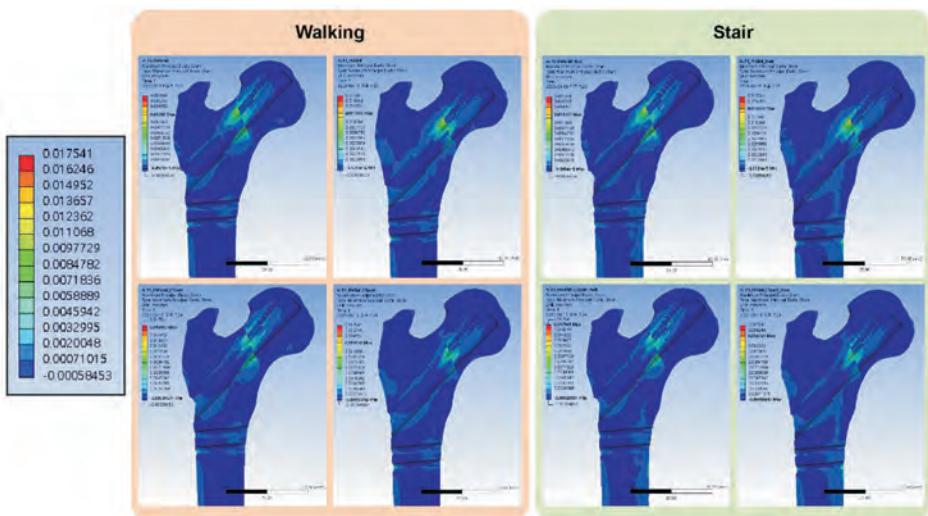

Fig. 4. Band graphs depicting the maximum principal strain of the femur in the normal walking (the 4 graphs on the left) and stair-climbing (the 4 graphs on the right) conditions. The graphs within each loading condition were arranged in the same sequence as in Fig 1. All graphs share the color legend.

distance were used to evaluate the mechanical stability at the fracture interface. Vertical movement relative to the surface is referred to as gap distance, whereas parallel movement along the surface is known as sliding distance. Interfragmentary compression was assessed by calculating the area ratio of the fracture site experiencing compressive forces exceeding 0 MPa and the peak compressive force observed at the fracture surface. ANSYS 2019 R3 mechanical software (ANSYS Inc.) was used for the solution of the finite element analysis. Figs. 4-8 depict the spatial distribution of values obtained from nodes through a bar graph, while Table 1 displays values derived from the elemental mean to differentiate the bone characteristics of each result element, which may result in variations in absolute values. Representative values of the elemental mean were recorded using Microsoft 365 Excel and Access (Microsoft), and differences of less than 5% were considered to be similar. When comparing the FNS-fixed models with and without an additional screw, the denominators of the ratios were derived from the corresponding parameters of the FNS-only model. When comparing the central and inferior trajectories, the denominators of the ratios were derived from the corresponding parameters of the central trajectory model.

RESULTS

Normal Walking Condition

Elements with a maximum principal strain > 1% and a minimum principal strain < –1% indicated the trabecular bone located in the narrow cleft between the anti-rotation screw and bolt, as well as under the bolt (Figs. 4 and 5,

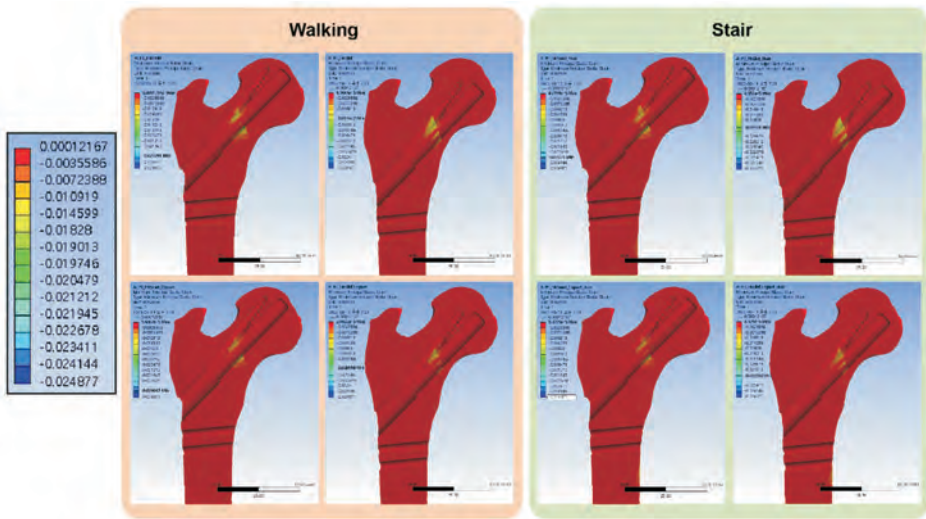

Fig. 5. Band graphs depicting the minimum principal strain of the femur in the normal walking (the 4 graphs on the left) and stair-climbing (the 4 graphs on the right) conditions. The graphs within each loading condition were arranged in the same sequence as in Fig 1. All graphs share the color legend.

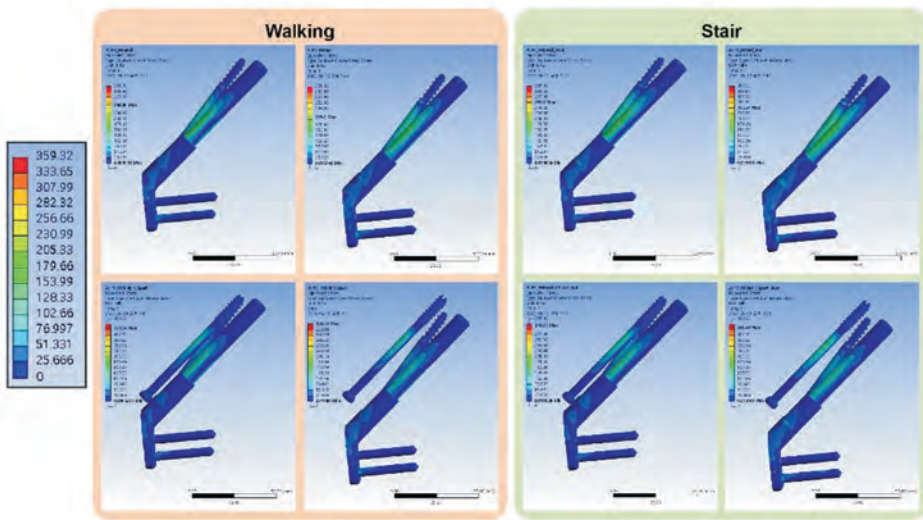

Fig. 6. Band graphs depicting von Mises stress of the implant in the normal walking (the 4 graphs on the left) and stair-climbing (the 4 graphs on the right) conditions. The graphs within each loading condition were arranged in the same sequence as in Fig 1. All graphs share the color legend.

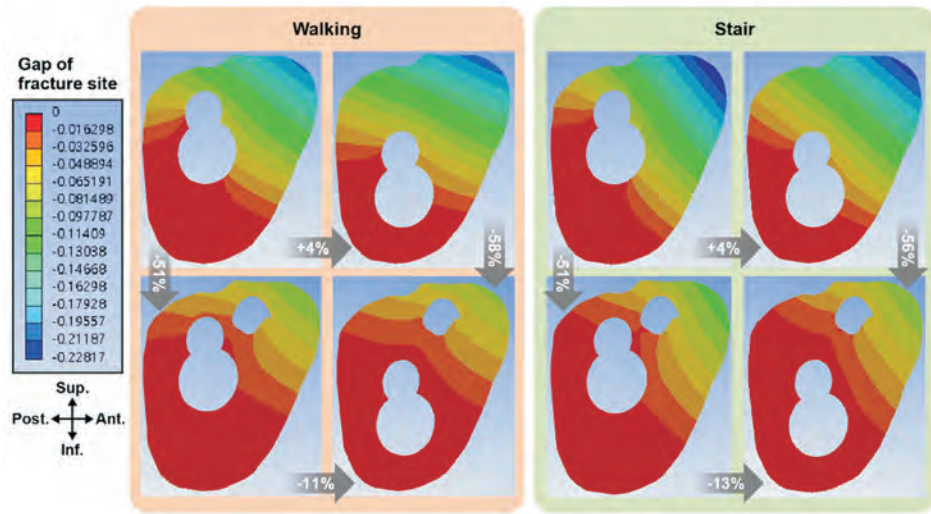

Fig. 7. Band graphs depicting gaps between fracture surfaces were drawn on the fracture surface in the normal walking (the 4 graphs on the left) and stair-climbing (the 4 graphs on the right) conditions. The graphs within each loading condition were arranged in the same sequence as in Fig 1. All graphs were aligned to share the color legend. While the gap is expressed as negative when the 2 surfaces move apart in the figure, it is interpreted as positive in Table 1 for clinical significance. To address visualization problems on screen, the graphs were realigned according to the directional indicators indicated in the figures, enabling easier comparison between models.

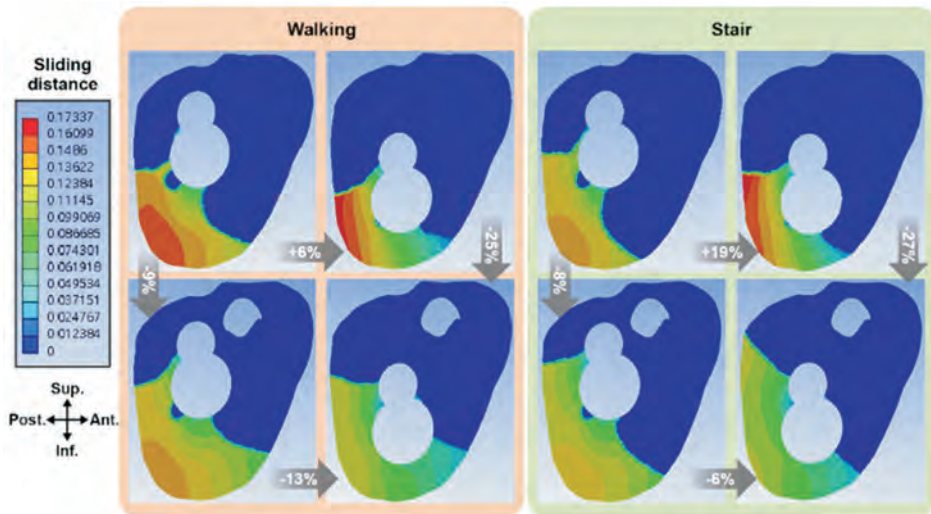

Fig. 8. Band graphs depicting sliding distances between fracture surfaces were drawn on the fracture surface in the normal walking (the 4 graphs on the left) and stair-climbing (the 4 graphs on the right) conditions. The graphs within each loading condition were arranged in the same sequence as in Fig 1. All graphs were aligned to share the color legend. While the gap is expressed as negative when the 2 surfaces move apart in the figure, it is interpreted as positive in Table 1 for clinical significance. To address visualization problems on screen, the graphs were realigned according to the directional indicators indicated in the figures, enabling easier comparison between models.

Table 1). The addition of a screw had mixed effects on the peak maximum and minimum principal strain of trabecular bone. However, it resulted in a consistent reduction in the volume of elements belonging to the trabecular bone that exhibited a maximum principal strain > 1% or a minimum principal strain < –1% (Table 1).

None of the cortical bone elements exceeded 1% of the maximum principal strain. The endosteal cortex in the inferior neck supporting the bolt in the "inferior FNS – screw" model had a peak minimum principal strain of –1.21% (Fig. 5, Table 1). The addition of a cannulated screw seemed to alleviate the minimum principal strain,

Table 1. Interfragmentary Motion and Stress on the Fracture Surface and Implant with or without an Additional Screw in the Pauwel Type III Femoral Neck Fracture Models Virtually Fixed with the Femoral Neck System

	Central bolt trajectory	Inferior bolt trajectory	Central bolt trajectory with a screw	Inferior bolt trajectory with a screw
Walking				
Peak maximum principal strain				
Cortical (%)	0.64	0.68	0.70	0.62
Volume of over 1% strain (μL)	0	0	0	0
Trabecular (%)	1.14	1.12	1.39	1.16
Volume of over 1% strain (μL)	1.0	0.8	0.4	0.1
Peak minimum principal strain				
Cortical (%)	–0.46	–1.21	–0.61	–0.85
Volume of under 1% strain (μL)	0	0.2	0	0
Trabecular (%)	–2.29	–1.68	–1.86	–1.73
Volume of under 1% strain (μL)	40.3	19.8	17.0	4.9
Implant stress (MPa)	268.9	215.7	338.0	359.3
Gap (mm)	0.198	0.206	0.098	0.087
Sliding (mm)	0.159	0.168	0.145	0.126
Interfragmentary compression				
Area ratio of compressive force > 0 MPa (%)	26.2	21.2	35.2	29.5
Peak compression (MPa)	13.8	14.5	11.4	12.0
Stair climbing				
Peak maximum principal strain				
Cortical (%)	0.79	0.87	0.63	0.85
Volume of over 1% strain (μL)	0	0	0	0
Trabecular (%)	1.15	1.24	1.56	1.23
Volume of over 1% strain (μL)	2.0	1.4	0.6	0.2
Peak minimum principal strain				
Cortical (%)	–1.07	–1.23	–1.05	–1.16
Volume of under 1% strain (μL)	0.1	0.9	0.3	1.3
Trabecular (%)	–2.24	–1.81	–1.95	–1.77
Volume of under 1% strain (μL)	34.2	22.9	14.8	6.5
Implant stress (MPa)	281.7	256.0	349.2	341.4
Gap (mm)	0.228	0.218	0.111	0.097
Sliding (mm)	0.146	0.173	0.134	0.126

Table 1. Continued

	Central bolt trajectory	Inferior bolt trajectory	Central bolt trajectory with a screw	Inferior bolt trajectory with a screw
Interfragmentary compression				
Area ratio of compressive force > 0 MPa (%)	24.8	21.4	34.3	30.1
Peak compression (MPa)	16.3	13.9	13.3	11.7

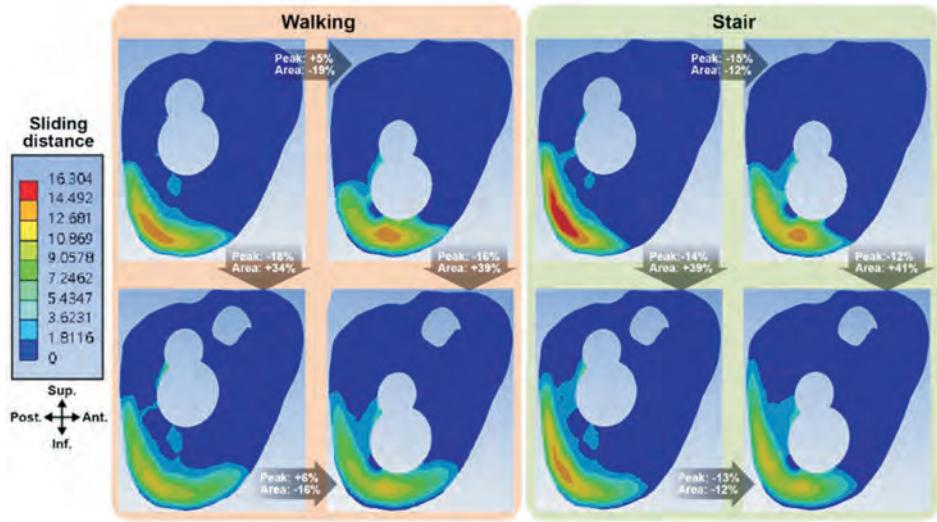

Fig. 9. Band graphs depicting interfragmentary compression between fracture surfaces were drawn on the fracture surface in the normal walking (the 4 graphs on the left) and stair-climbing (the 4 graphs on the right) conditions. The graphs within each loading condition were arranged in the same sequence as in Fig 1. All graphs were aligned to share the color legend. While the gap is expressed as negative when the 2 surfaces move apart in the figure, it is interpreted as positive in Table 1 for clinical significance. To address visualization problems on screen, the graphs were realigned according to the directional indicators indicated in the figures, enabling easier comparison between models.

as its absolute value decreased to 0.85% (Fig. 5, Table 1). No other models had elements with a maximum principal strain > 1% and a minimum principal strain < –1% in the cortical bone. The peak VMS of the implants ranged from 216 to 359 MPa. Adding a screw to the FNS resulted in an increase in VMS compared to the corresponding FNS-only models. VMS in the central and inferior trajectory models increased by 25.7% and 66.6%, respectively, with the addition of the screw. The highest peak VMS was still lower than the yield strength of the titanium alloy, which is 800 MPa (Fig. 6, Table 1).[18]

The "inferior FNS – screw" model had a comparable gap and a 6.0% larger sliding distance between fracture fragments compared to the "central FNS – screw" model. The addition of a cannulated screw to the model with a bolt in the central trajectory halved the gap between fracture fragments by 50.6% and decreased the sliding distance between fragments by 8.6%. The addition of a cannulated screw to the "inferior FNS" model decreased the gap by 57.9% and the sliding distance between fragments by 25.0%. Although the gap and sliding distance in the "inferior FNS – screw" model were larger than those in the "central FNS – screw" model by 4.0% and 6.0%, respectively, the relationship was reversed after the addition of a cannulated screw. In this case, the "inferior FNS + screw" model demonstrated a smaller gap and sliding distance as compared to the "central FNS + screw" model, with reductions of 11.3% and 13.1%, respectively. (Figs. 7 and 8, Supplementary Figs. 1 and 2, Table 1).

The "inferior FNS – screw" model had 5% higher peak interfragmentary compression and a 19% lower area ratio of the fracture site with compressive force exceeding 0 MPa compared to the "central FNS – screw" model. The addition of a cannulated screw to the model with a bolt in the central trajectory reduced the peak interfragmentary compression by 18% and increased the area ratio of the fracture site with compressive force exceeding 0 MPa by 34%. The addition of a cannulated screw to the model with

a bolt in the inferior trajectory reduced the peak interfragmentary compression by 16% and increased the area ratio of the fracture site with compressive force exceeding 0 MPa by 39% (Fig. 9, Supplementary Fig. 3, Table 1).

Stair-Climbing Condition

The trabecular bone located in the narrow cleft between the anti-rotation screw or under the plate that supports the bolt exhibited an absolute magnitude of strain > 1% under the stair-climbing load (Figs. 4 and 5, Table 1). The addition of a screw had mixed effects on the peak maximum and minimum principal strain of trabecular bone. However, it resulted in a reduction in the volume of elements belonging to the trabecular bone that exhibited a maximum principal strain > 1% or a minimum principal strain < –1% (Table 1).

In all the models, the medial cortex of the femoral neck exceeded –1% of the minimum principal strain, ranging from –1.07% to –1.23% (Fig. 5, Table 1). The volume of cortical bone elements with an absolute value above 1% remained less than 1.3 μL. The peak VMS of the implants ranged from 256 to 349 MPa. The highest peak VMS was still lower than the yield strength of the titanium alloy (Fig. 6, Table 1). The addition of a screw to FNS led to a rise in VMS as compared to the FNS-only models. The addition of a screw increased the VMS in the central and inferior trajectory models by 24.0% and 33.3%, respectively.

Adding a cannulated screw to the inferior FNS model halved the gap between fracture fragments and decreased the sliding distance between fragments by 7.9%. Adding a cannulated screw to the inferior FNS model decreased the gap by 55.7% and the sliding distance between fragments by 27.2%. Without the additional screw, the "inferior FNS – screw" model had a comparable gap and approximately 19.0% more sliding between fracture fragments than the "central FNS – screw" model (Figs. 7 and 8, Supplementary Figs. 1 and 2, Table 1). The addition of a cannulated screw made the gap difference significant, reaching a 12.8% difference with a smaller gap in the "inferior FNS + screw" model. The addition of the screw reversed the relationship of sliding distance, as the "inferior FNS + screw" model had a smaller sliding distance than the "central FNS + screw" model by 5.9%.

During stair-climbing, the "inferior FNS – screw" model had 15% lower peak interfragmentary compression and a 12% lower area ratio of the fracture site with compressive force exceeding 0 MPa compared to the "central FNS – screw" model. The addition of a cannulated screw to the model with a bolt in the central trajectory reduced the peak interfragmentary compression by 14% and increased the area ratio of the fracture site with compressive force exceeding 0 MPa by 39%. The addition of a cannulated screw to the model with a bolt in the inferior trajectory reduced the peak interfragmentary compression by 12% and increased the area ratio of the fracture site with compressive force exceeding 0 MPa by 41% (Fig. 9, Supplementary Fig. 3, Table 1).

DISCUSSION

This study employed finite element analysis to examine the biomechanical effects of adding a screw to FNS for the fixation of Pauwel type III femoral neck fractures. The addition of a screw either maintained or decreased bone strain, while reducing the fracture gap and sliding distance, thereby leading to a comprehensive improvement in stability, regardless of whether the FNS bolt trajectory passes through the central or inferior trajectory. While FNS in the central trajectory provides better stability than FNS in the inferior trajectory without an additional screw, the addition of an extra screw reversed the relationship, with the greater improvement in stability observed in the inferior trajectory model.[13,21,27]

Adding a screw in both trajectories had a beneficial impact, reducing the gap between fractures and the distance of sliding with the alleviation of bone strain. This led to increased stability at the fracture site. These results are in line with a prior finite element analysis conducted by Kuang et al.,[28] where they compared 3 fixation models: the central trajectory, the lower trajectory, and the lower trajectory of the bolt combined with a cannulated screw. Although the study had certain limitations, such as the use of a 3D model that did not consider the surgical procedure, the exclusion of muscle load in the loading conditions, and the assumption of bone as a homogeneous material, it supports the idea that the addition of a cannulated screw enhances stability at the fracture surface. The idea of adding a screw to the FNS is currently being tried in the clinical field. Recent clinical study assessed the addition of a screw to FNS with retrospective manner.[29] By combining an additional screw with FNS, Su et al.[29] reported favorable outcomes in 129 young adults with femoral neck fractures.

Previous mechanical studies utilizing a finite element model to assess the stability of femoral neck fractures treated with the FNS alone have indicated that the FNS with a central bolt trajectory exhibited slightly better stability at the fracture site compared to the inferior trajectory.[13,21,27] However, the addition of a screw was observed to result in a greater enhancement of fracture stability when the FNS bolt passed through the inferior trajectory, surpassing the stability achieved with the central bolt tra-

jectory model. The previous finite element analysis conducted by Kuang et al.[28] did not include a model with an additional screw in the central trajectory, thus limiting the exploration of this relationship. In this study, the effects of screw addition were demonstrated in both trajectories, highlighting its efficacy in both cases and particularly indicating higher stability in the inferior trajectory.

Research examining the biomechanical consequences of screw arrangement in multiple screw techniques for femoral neck fractures consistently shows that greater spacing between screws results in improved stability.[3] This can be attributed to the acquisition of cortical support with larger spacing and the longer lever arm provided by the increased distance between each screw, effectively addressing rotational loads. Taking these insights into account, the effects of FNS trajectory and the addition of a screw can be interpreted in terms of cortical support and increased lever arm for rotational loads. In this context, by placing the FNS bolt in the inferior trajectory, a larger spacing between the FNS and the additional screw was achieved. This larger spacing facilitated cortical support and created a longer lever arm, resulting in greater stability. In comparison, adding a screw to the FNS in the central trajectory did not provide the same degree of spacing, cortical support, and lever arm length, thereby yielding a lesser level of stability compared to those with the inferior trajectory.

The addition of an extra screw demonstrated that it could create a favorable mechanical environment for fracture healing at the fracture site. The increased area ratio of compressive force in models with the additional screw indicates enhanced stability at the fracture site. This improvement in compressive force distribution is crucial for promoting fracture healing as it helps maintain bone contact and reduces the likelihood of fragment separation. Additionally, while the peak compressive forces were slightly lower in the screw-added models, the distribution of forces was more uniform, reducing localized stress concentrations. These findings suggest that the addition of a screw disperses compressive forces across a wider area of the fracture surface in femur neck fractures fixed with FNS, creating a more favorable mechanical environment for bone healing under both normal walking and stair-climbing conditions. Considering that cyclic compressive loads are beneficial for fracture healing, the wider distribution of compressive loads under weight-bearing conditions further supports improved conditions for fracture union.[30]

While our comparative analysis provided interesting results, it is important to acknowledge the limitations of the present study. Finite element analysis relies on simplifying assumptions, which may raise concerns about the clinical applicability of the results. The femur models were generated from CT images of an elderly patient, and the material properties were assigned based on the grey values of the corresponding voxels, while assuming isotropic and elastic properties for the bone. Assigning material properties based on CT values may help bridge the gap between simulations and real-world scenarios. It is important to recognize that numerous factors, including patient-, surgeon-, and fracture-related factors, are known to influence fracture treatment outcomes. In this analysis, our focus was specifically on evaluating the performance of the FNS and an additional screw. We assumed that all other surgical objectives, such as fracture reduction, were successfully achieved, thus, there was no gap at the fracture interface before loading. We believe that the qualitative insights gained from this comparative analysis will enhance our understanding of the FNS.

In conclusion, the present finite element analysis investigated the effects of adding a screw to the FNS for Pauwel type III femoral neck fractures. The addition of a screw resulted in a reduction of the fracture gap, sliding distance, and peak interfragmentary compression and an increase in the area ratio of interfragmentary compression under both walking and stair-climbing loads, regardless of whether the FNS bolt trajectory passed through the central or inferior path. This suggests that the extra screw may provide a better mechanical environment for fracture healing. These findings need to be further validated through additional biomechanical and clinical investigations.

CONFLICT OF INTEREST

No potential conflict of interest relevant to this article was reported.

ACKNOWLEDGEMENTS

We would like to express our gratitude to Dentium (Seoul, Korea) for their assistance with the reconstruction of the finite element models and virtual surgery using MIMICS Research 22.0, 3-matic 14, NRecon, and Solidworks 2019. Additionally, we would like to thank Tae Sung S&E (Seoul, Korea) for their technical support with the operation of Ansys software, and TDM (Seoul, Korea) for providing the 3-dimensional computer-aided design (CAD) file of a cannulated screw with a 6.5 thread diameter.

This research was supported by a grant of the Korea Health Technology R&D Project through the Korea Health Industry Development Institute (KHIDI), funded by the Ministry of Health & Welfare, Republic of Korea

(No. HI22C0494), and the National Research Foundation of Korea (NRF) grant funded by the Korea government (MSIT) (No. 2022R1G1A1003299). This work was supported by the new faculty research fund of Ajou University School of Medicine. No benefits in any form have been received or will be received from a commercial party related directly or indirectly to the subject of this article.

ORCID

Yonghan Cha https://orcid.org/0000-0002-7616-6694
Sunghoon Park https://orcid.org/0000-0003-0844-0521
Chang-Ho Jung https://orcid.org/0000-0001-8318-4447
Jin-Woo Kim https://orcid.org/0000-0003-0186-5834
Jun-Il Yoo https://orcid.org/0000-0002-3575-4123
Jung-Taek Kim https://orcid.org/0000-0003-4243-5793
Yongho Jeon https://orcid.org/0000-0002-0183-8652
Kyeong Jin Han https://orcid.org/0000-0002-8853-3754

SUPPLEMENTARY MATERIAL

Supplementary material is available in the electronic version of this paper at the CiOS website, www.ecios.org.

REFERENCES

1. Fischer H, Maleitzke T, Eder C, Ahmad S, Stockle U, Braun KF. Management of proximal femur fractures in the elderly: current concepts and treatment options. Eur J Med Res. 2021;26(1):86.
2. Cha YH, Yoo JI, Hwang SY, et al. Biomechanical evaluation of internal fixation of Pauwels type III femoral neck fractures: a systematic review of various fixation methods. Clin Orthop Surg. 2019;11(1):1-14.
3. Zhu Q, Shi B, Xu B, Yuan J. Obtuse triangle screw configuration for optimal internal fixation of femoral neck fracture: an anatomical analysis. Hip Int. 2019;29(1):72-6.
4. Chang JZ, Xiao YP, Li L, Bei MJ. The efficacy of dynamic compression locking system vs. dynamic hip screw in the treatment of femoral neck fractures: a comparative study. BMC Musculoskelet Disord. 2022;23(1):661.
5. Nan C, Ma L, Liang Y, Li Y, Ma Z. Mechanical effects of sagittal variations on Pauwels type III femoral neck fractures treated with Femoral Neck System (FNS). BMC Musculoskelet Disord. 2022;23(1):1045.
6. Park JW, Lee YK, Kim HS, Kim JK, Ha YC, Koo KH. Incidence and risk factors of short axial length of the proximal femur: a caution in the use of femoral neck system in patients with garden type I/II femoral neck fractures. Clin Orthop Surg. 2023;15(3):388-94.
7. Bonnaire FA, Weber AT. Analysis of fracture gap changes, dynamic and static stability of different osteosynthetic procedures in the femoral neck. Injury. 2002;33 Suppl 3:C24-32.
8. Cha Y, Song JU, Yoo JI, et al. Improved control over implant anchorage under the use of the femoral neck system for fixation of femoral neck fractures: a technical note. BMC Musculoskelet Disord. 2021;22(1):621.
9. Cha Y, Chung JY, Jung CH, et al. Pre-sliding of femoral neck system improves fixation stability in pauwels type III femoral neck fracture: a finite element analysis. BMC Musculoskelet Disord. 2023;24(1):506.
10. DePuy Synthes. Surgical technique of Femoral Neck System [Internet]. DePuy Synthes; 2024 [cited 2024 May 5]. Available from: https://www.jnjmedtech.com/en-US/product/femoral-neck-system-fns
11. Bergmann G, Graichen F, Rohlmann A. Hip joint loading during walking and running, measured in two patients. J Biomech. 1993;26(8):969-90.
12. Sheehan SE, Shyu JY, Weaver MJ, Sodickson AD, Khurana B. Proximal femoral fractures: what the orthopedic surgeon wants to know. Radiographics. 2015;35(5):1563-84.
13. Jung CH, Cha Y, Yoon HS, et al. Mechanical effects of surgical variations in the femoral neck system on Pauwels type III femoral neck fracture: a finite element analysis. Bone Joint Res. 2022;11(2):102-11.
14. Gujar RA, Warhatkar HN. Estimation of mass apparent density and Young's modulus of femoral neck-head region. J Med Eng Technol. 2020;44(7):378-88.
15. Lee PY, Lin KJ, Wei HW, et al. Biomechanical effect of different femoral neck blade position on the fixation of inter-

trochanteric fracture: a finite element analysis. Biomed Tech (Berl). 2016;61(3):331-6.

16. Morgan EF, Bayraktar HH, Keaveny TM. Trabecular bone modulus-density relationships depend on anatomic site. J Biomech. 2003;36(7):897-904.
17. Taddei F, Schileo E, Helgason B, Cristofolini L, Viceconti M. The material mapping strategy influences the accuracy of CT-based finite element models of bones: an evaluation against experimental measurements. Med Eng Phys. 2007; 29(9):973-9.
18. ASTM International. Standard specification for wrought titanium-6aluminum-7niobium alloy for surgical implant applications (UNS R56700) [Internet]. ASTM International; 2016 [cited 2024 May 5]. Available from: https://www.astm.org/f1295-16.html
19. Morlock M, Schneider E, Bluhm A, et al. Duration and frequency of every day activities in total hip patients. J Biomech. 2001;34(7):873-81.
20. Heller MO, Bergmann G, Kassi JP, Claes L, Haas NP, Duda GN. Determination of muscle loading at the hip joint for use in pre-clinical testing. J Biomech. 2005;38(5):1155-63.
21. Jung CH, Cha Y, Chung JY, et al. Trajectory of bolt and length of plate in femoral neck system determine the stability of femur neck fracture and risk of subsequent subtrochanteric fracture: a finite element analysis. BMC Musculoskelet Disord. 2023;24(1):465.
22. Nalla RK, Kinney JH, Ritchie RO. Mechanistic fracture criteria for the failure of human cortical bone. Nat Mater. 2003; 2(3):164-8.
23. Cilla M, Checa S, Preininger B, et al. Femoral head necrosis: a finite element analysis of common and novel surgical techniques. Clin Biomech (Bristol, Avon). 2017;48:49-56.
24. Goffin JM, Pankaj P, Simpson AH. The importance of lag screw position for the stabilization of trochanteric fractures with a sliding hip screw: a subject-specific finite element study. J Orthop Res. 2013;31(4):596-600.
25. Goffin JM, Pankaj P, Simpson AH. A computational study on the effect of fracture intrusion distance in three- and four-part trochanteric fractures treated with Gamma nail and sliding hip screw. J Orthop Res. 2014;32(1):39-45.
26. Pistoia W, van Rietbergen B, Lochmuller EM, Lill CA, Eckstein F, Ruegsegger P. Estimation of distal radius failure load with micro-finite element analysis models based on three-dimensional peripheral quantitative computed tomography images. Bone. 2002;30(6):842-8.
27. Kim JT, Jung CH, Shen QH, et al. Mechanical effect of different implant caput-collum-diaphyseal angles on the fracture surface after fixation of an unstable intertrochanteric fracture: a finite element analysis. Asian J Surg. 2019;42(11):947-56.
28. Kuang X, Jian G, Xie D, Chen X, Liu H. Choose the appropriate implantation position of the Femoral Neck System in the femoral neck: a finite-element analysis. Eur J Trauma Emerg Surg. 2023;49(4):1845-53.
29. Su M, He Z, Huang N, Lin X, Fang K, Dai Z. Superior short-term outcomes of FNS in combination with a cannulated screw in treating femoral neck fractures. BMC Musculoskelet Disord. 2023;24(1):823.
30. Ma Q, Miri Z, Haugen HJ, Moghanian A, Loca D. Significance of mechanical loading in bone fracture healing, bone regeneration, and vascularization. J Tissue Eng. 2023;14: 20417314231172573.